Chapter 1

Theory of Excitons and Excitonic Quasimolecules Formed from Spatially Separated Electrons and Holes in Quasi-Zero-Dimensional Nanostructures

Sergey I. Pokutnyi and Włodzimierz Salejda

Additional information is available at the end of the chapter

http://dx.doi.org/10.5772/60591

Abstract

The theory of an exciton formed from a spatially separated electron and a hole is developed within the framework of the modified effective mass method. The effect of significantly increasing the exciton binding energy in quantum dots of zinc selenide, synthesized in a borosilicate glass matrix and relative to that in a zinc selenide single crystal is revealed. It is shown that the short-wavelength shift of the peak of the low-temperature luminescence spectrum of samples containing zinc selenide quantum dots, observed under experimental conditions, is caused by quantum confinement of the ground-state energy of the exciton with a spatially separated electron and hole.

A review devoted to the theory of excitonic quasimolecules (biexcitons) (made up of spatially separated electrons and holes) in a nanosystem that consists of ZnSe quantum dots synthesized in a borosilicate glass matrix is developed within the context of the modified effective mass approximation. It is shown that biexciton (exciton quasimolecule) formation has a threshold character and is possible in a nanosystem, where the spacing between quantum dots' surfaces is larger than a certain critical arrangement. An analogy of the spectroscopy of the electronic states of superatoms (or artificial atoms) and individual alkali metal atoms theoretically predicted a new artificial atom that was similar to the new alkali metal atom.

Keywords: Excitons, exciton binding energy, quantum dots, excitonic quasimolecules, spatially separated electrons and holes, superatoms

1. Introduction

Quasi-zero-dimensional semiconductor nanosystems consisting of spherical semiconductor nanocrystals, i.e., quantum dots with radii of a =1-10 nm and containing cadmium sulphide and selenide, gallium arsenide, germanium, silicon, and zinc selenide in their volume, and synthesized in a borosilicate glass matrix currently attract particular research attention due to their unique photoluminescent properties, i.e., the ability to efficiently emit light in the visible or near infrared ranges at room temperature [1-10]. The optical and electro-optical properties of such quasi-zero dimensional nanosystems are to a large extent controlled by the energy spectrum of the spatially confined electron-hole pair (exciton) [4-16].

In most theoretical models for calculating the energy spectra of quasiparticles in quantum dots (QDs), the effective mass approximation is used, which was considered applicable for QDs by analogy with bulk single crystals [11-13]. However, the problem concerning the applicability of the effective mass approximation to the description of semiconductor QDs remains unsolved [4-18].

In [14], a new modified effective mass method is proposed to describe the exciton energy spectrum in semiconductor QDs with radii of $a \approx a_{ex}$ (a_{ex} is the exciton Bohr radius in the semiconductor material contained in the QD volume). It was shown that, within a model in which the QD is represented as an infinitely deep potential well, the effective mass approximation can be applied to the description of an exciton in QDs with radii a comparable to the exciton Bohr radius a_{ex}, assuming that the reduced effective exciton mass is a function of the radius a, $\mu = \mu(a)$.

In the adiabatic approximation and within the modified effective mass method [14], an expression for the binding energy of an exciton, whose electron and hole move within the semiconductor QD volume, was derived in [15]. In [15], the effect of significantly increasing the exciton binding energy in cadmium selenide and sulphide QDs with radii a, comparable to the exciton Bohr radii a_{ex} and relative to the exciton- binding energy in cadmium selenide and sulphide single crystals (by factors of 7.4 and 4.5, respectively) was also detected.

In the experimental study [7], it was found that excess electrons produced during interband excitation of the cadmium sulphide QD had a finite probability of overcoming the potential barrier and penetrating into the borosilicate glass matrix, into which the QD is immersed. In experimental studies [10, 19] (as well as in [7]) using glass samples with cadmium-sulphide and zinc selenide QDs, it was found that the electron can be localized in the polarization well near the outer QD surface, while the hole moves within the QD volume.

In [10, 19], the optical properties of borosilicate glass samples containing QD zinc selenide were experimentally studied. The average radii of such QDs were in the range $a \approx$ 2.0-4.8 nm. In this case, the values of a are comparable to the exciton Bohr radius $a_{ex} \approx$ 3.7 nm in a ZnSe single crystal. At low QD concentrations, when the optical properties of the samples are mainly controlled by those of individual QDs in the borosilicate glass matrix, a shift of the peak of the

http://dx.doi.org/10.5772/60591

low temperature luminescence spectrum to the short wavelength region (with respect to the band gap E_g of the zinc selenide-single crystal) was observed. The authors of [10] assumed that this shift was caused by quantum confinement of the energy spectra of the electron and the hole localized near the spherical surface of the QD. In this case, the following problem remained open: the quantum confinement of the state of which electron and hole (the hole moving in the QD volume and the electron localized at the outer spherical QD-dielectric matrix interface or the electron and hole localized in the QD volume) caused such a shift in the luminescence spectrum peak?

The use of semiconductor nanosystems as the active region of nanolasers is prevented by the low binding energy of the QD exciton [8, 9, 13]. Therefore, studies directed at the search for nanostructures in which a significant increase in the binding energy of QD excitons can be observed are of importance.

Currently, the theory of exciton states in quasi- zero- dimensional semiconductor nanosystems has not been adequately studied. In particular, no theory exists for an exciton with a spatially separated electron and hole in quasi- zero- dimensional nanosystems. Therefore, in this study, we developed the theory of an exciton formed from a spatially separated electron and hole (the hole is in the semiconductor QD volume and the electron is localized at the outer spherical surface of the QD-dielectric matrix interface) [20-22]. It was shown that the short wavelength shift of the peak of the low temperature luminescence spectrum of samples containing zinc selenide QDs, observed under the experimental conditions of [10], was caused by quantum confinement of the ground state energy of the exciton with a spatially separated electron and hole. The effect of significantly increasing the binding energy of an exciton (with a spatially separated electron and hole) in a nanosystem containing zinc selenide QDs, compared with the binding energy of an exciton in a zinc selenide single crystal (by a factor of 4.1-72.6), was detected [20-22].

In [10, 19], a shift of the spectral peak of the low temperature luminescence was also observed for samples with a QD concentrations from x = 0.003-1%. It was noted [10, 19] that at such a QD content in the samples, the interaction between charge carriers localized above the QD surfaces must be taken into account. Therefore, in [23, 24], we develop the theory of excitonic quasimolecules (biexcitons) (formed from spatially separated electrons and holes) in a nanosystem, which consists of ZnSe QDs synthesized in a borosilicate glass matrix.

2. Spectroscopy of excitons in Quasi - Zero - Dimensional nanosystems

Let us consider the simple model of a quasi-zero-dimensional system, i.e., a neutral spherical semiconductor QD of the radius a, which contains semiconductor material with the permittivity ε2 in its volume, surrounded by a dielectric matrix with permittivity ε_1. A hole h with the effective mass m_h moves in the QD volume, while an electron e with the effective mass $m_e^{(1)}$ lies in the matrix (r_e and r_h are the distances from the QD centre to the electron and hole). Let

us assume that the QD valence band is parabolic. Let us also assume that there is an infinitely high potential barrier at the spherical QD-dielectric matrix interface; therefore, the hole *h* cannot leave the QD volume and the electron *e* cannot penetrate into the QD volume in the model under study [20-22].

The characteristic dimensions of the problem are the quantities:

$$a_h = \varepsilon_2 \hbar^2 / m_h e^2, \quad a_{ex} = \varepsilon_2 \hbar^2 / \mu e^2, \quad a_e = \varepsilon_1 \hbar^2 / m_e^{(1)} e^2, \tag{1}$$

where a_h and a_{ex} are the hole and exciton Bohr radii in the semiconductor with the permittivity ε2, *e* is the elementary charge, $\mu = m_e^{(2)} m_h / (m_e^{(2)} + m_h)$ is the reduced effective mass of the exciton, $m_e^{(2)}$ is the effective mass of an electron in the semiconductor with permittivity ε_2 and a_e is the electron Bohr radius in the dielectric matrix with the permittivity ε1. The fact that all characteristic dimensions of the problem are significantly larger than the interatomic distances a_0,

$$a, a_e, a_h, a_{ex} >> a_0$$

allows us to consider the electron and hole motion in the quasi-zero-dimensional nanosystem in the effective mass approximation [11-13].

We analysed the conditions of carrier localization in the vicinity of a spherical dielectric particle of the radius *a* with the permittivity ε_2 in [25-27]. In this instance, the problem of the field induced by the carrier near a dielectric particle immersed in a dielectric medium with the permittivity ε_1 was solved in a final analytical form and analytical expressions for the potential energy of the interaction of the carrier with the spherical interface of two media are presented.

Solving the Poisson equation with usual electrostatic boundary conditions

$$\begin{aligned} \phi(r', j \mid \boldsymbol{r}, i)\big|_{r'=a} &= \phi(\boldsymbol{r}', j)\big|_{r'=a}, \\ \varepsilon_1 \frac{\partial \phi(\boldsymbol{r}', j \mid \boldsymbol{r}, i)}{\partial \boldsymbol{r}'}\Big|_{r'=a} &= \varepsilon_2 \frac{\partial \phi(\boldsymbol{r}', j)}{\partial \boldsymbol{r}'}\Big|_{r'=a}, \end{aligned} \tag{2}$$

the potential $\varphi(\boldsymbol{r}', j \mid \boldsymbol{r}, i) \mid$ at the observation point $\boldsymbol{r}'$ in a medium with the permittivity ε_j, induced by the charge *e* at the point $\boldsymbol{r}$ in a medium with the permittivity ε_i, can be presented as a sum of the potentials induced by the image point charge $e'(\boldsymbol{r}_{ij} \mid \boldsymbol{r})$ at the point $\boldsymbol{r}_{ij} = (a/r)^2 \boldsymbol{r} \delta_{ij} + \boldsymbol{r}(1 - \delta ij)$ and the linear distribution with the density $\rho_{ij}(y, r)$ of the image charge along a straight line passing through the centre of the dielectric particle with the radius *a* and the charge at the point $\boldsymbol{r}$ [25-27]:

http://dx.doi.org/10.5772/60591

$$\phi(\boldsymbol{r}', j \mid \boldsymbol{r}, i) = \frac{e}{\varepsilon_j \mid \boldsymbol{r}' - \boldsymbol{r} \mid} + \frac{e'(\boldsymbol{r_{ij}} \mid \boldsymbol{r})}{\varepsilon_j \mid \boldsymbol{r}' - \boldsymbol{r_{ij}} \mid} + \frac{1}{\varepsilon_j} \int_0^\infty \frac{dy \rho_{ij}(y, \boldsymbol{r})}{\mid \boldsymbol{r}' - y(\boldsymbol{r}/r) \mid}$$

where

$$\mathrm{r}_{11} = (a^2/r^2)\boldsymbol{r}, e'(\mathrm{r}_{11} \mid \mathrm{r}) = -\beta(a/r)e \qquad \text{a}$$

$$\rho_{11}(y,r) = \beta\alpha\left(a^2/ry\right)^{(1-\alpha)}(e/a)\theta((a^2/r) - y);$$

$$\mathrm{r}_{22} = \left(a^2/r^2\right)\mathrm{r}, e'\left(\mathrm{r}_{22} \mid \mathrm{r}\right) = \beta\left(a/r\right)e \qquad \text{b} \qquad (3)$$

$$\rho_{22}(y,r) = \beta\left(1-\alpha\right)\left(a^2/ry\right)^{\alpha}\left(e/a\right)\theta\left(y - \left(a^2/r\right)\right);$$

$$r_{12} = r, e'(\mathrm{r}_{12} \mid \mathrm{r}) = \beta e \qquad \text{c}$$

$$\rho_{12}(y,r) = \beta(1-\alpha)(r/y)^{\alpha}(e/r)\theta(y-r);$$

$$r_{21} = r, e'\left(r_{12} \mid r\right) = -\beta e \qquad \text{d}$$

$$\rho_{21}(y,r) = \beta\alpha\left(r/y\right)^{(1-\alpha)}(e/r)\theta\left(r-y\right)$$

where $\theta(x)$ is the Heaviside unit-step function,

$$\beta = \frac{\left(\varepsilon_2 - \varepsilon_1\right)}{\left(\varepsilon_2 + \varepsilon_1\right)}, \alpha = \frac{\varepsilon_1}{\left(\varepsilon_2 + \varepsilon_1\right)} \qquad (4)$$

Using expressions (3)-(3d), the energy $U(\mathrm{r}_e, \mathrm{r}_h, a)$ of the polarization interaction of the electron and hole with the spherical QD-matrix interface at the relative permittivity $\varepsilon = (\varepsilon_2/\varepsilon_1) \gg 1$ can be presented as an algebraic sum of the energies of the interaction of the hole and electron with self- $V_{h\,h'}(r_h, a)$, $V_{ee'}(r_e, a)$ and "foreign" $V_{eh'}(\boldsymbol{r}_e, \boldsymbol{r}_h, a)$, $V_{he'}(\boldsymbol{r}_e, \boldsymbol{r}_h, a)$ images, respectively [15, 16, 26-28]:

$$U(\mathrm{r_e}, \mathrm{r_h}, a, \varepsilon) = V_{hh'}\left(r_h, a, \varepsilon\right) + V_{ee'}\left(r_e, a, \varepsilon\right) + V_{eh'}\left(\mathrm{r_e}, \mathrm{r_h}, a, \varepsilon\right) + V_{he'}\left(\mathrm{r_e}, \mathrm{r_h}, a, \varepsilon\right), \qquad (5)$$

where

$$V_{hh'}\left(r_h, a, \varepsilon\right) = \frac{e^2\beta}{2\varepsilon_2 a}\left(\frac{a^2}{a^2 - r_h^{\,2}} + \varepsilon\right), \qquad (6)$$

$$V_{ee'}\left(r_e, a, \varepsilon\right) = -\frac{e^2\beta}{2\varepsilon_1 a} \cdot \frac{a^4}{r_e^2(r_e^2 - a^2)}, \qquad (7)$$

$$V_{he'}\left(\mathrm{r_e},\mathrm{r_h},a,\varepsilon\right)=\frac{e^2\beta}{2\varepsilon_2 a}\cdot\frac{a^2}{r_e\left|\mathrm{r_h}-\left(a/r_e\right)^2\mathrm{r_e}\right|}, \tag{8}$$

$$V_{eh'}\left(\mathrm{r_e},\mathrm{r_h},a,\varepsilon\right)=-\frac{e^2\beta}{2\varepsilon_1 a}\cdot\frac{a^2}{r_h\left|\mathrm{r_e}-\left(a/r_h\right)^2\mathrm{r_h}\right|}. \tag{9}$$

In the studied simple model of a quasi-zero-dimensional nanostructure within the above approximations and in the effective mass approximation using the triangular coordinate system [14-16], $r_e = |\boldsymbol{r}_e|$, $r_h = |\boldsymbol{r}_h|$, $r = |\boldsymbol{r}_e - \boldsymbol{r}_h|$, with the origin at the centre of the QD, the exciton Hamiltonian (with a spatially separated hole moving within the QD volume and an electron in the dielectric matrix) takes the following form [20-22, 29-32]:

$$\begin{aligned}H\left(\mathrm{r_e},\mathrm{r_h},\mathrm{r},a\right)=&-\frac{\hbar^2}{2m_e^{(1)}}\left(\frac{\partial^2}{\partial r_e^2}+\frac{2}{r_e}\cdot\frac{\partial}{\partial r_e}+\frac{r_e^2-r_h^2+r^2}{r_e r}\cdot\frac{\partial^2}{\partial r_e\partial r}\right)-\\&-\frac{\hbar^2}{2m_h}\left(\frac{\partial^2}{\partial r_h^2}+\frac{2}{r_h}\cdot\frac{\partial}{\partial r_h}+\frac{r_h^2-r_e^2+r^2}{r_h r}\cdot\frac{\partial^2}{\partial r_h\partial r}\right)-\frac{\hbar^2}{2\mu_0}\left(\frac{\partial^2}{\partial r^2}+\frac{2}{r}\cdot\frac{\partial}{\partial r}\right)+\\&+V_{eh}\left(\mathrm{r}\right)+U\left(\mathrm{r_e},\mathrm{r_h},a,\varepsilon\right)+V_e\left(r_e\right)+V_h\left(r_h\right)+E_g,\end{aligned} \tag{10}$$

where the first three terms are the operators of the electron, hole and exciton kinetic energy, Eg is the band gap in the semiconductor with the permittivity ε_2 and $\mu_0 = m_e^{(1)} m_h / (m_e^{(1)} + m_h)$ is the reduced effective mass of the exciton (with a spatially separated hole and electron). In the exciton Hamiltonian (10), the polarization interaction energy $U(\mathbf{r}_e, \mathbf{r}_h, a, \varepsilon)$ (5) is defined by formulas (6)-(9) and the electron-hole Coulomb interaction energy $Veh(r)$ is described by the following formula:

$$V_{eh}\left(r\right)=-\frac{1}{2}\left(\frac{1}{\varepsilon_1}+\frac{1}{\varepsilon_2}\right)\frac{e^2}{r} \tag{11}$$

In the exciton Hamiltonian (10), the potentials

$$\begin{aligned}V_h\left(r_h\right)&=\begin{cases}0, & r_h\le a\\ \infty, & r_h>a\end{cases},\\V_e\left(r_e\right)&=\infty,\quad r_e\le a\end{aligned} \tag{12}$$

describe the quasiparticle motion using the models of an infinitely deep potential well.

http://dx.doi.org/10.5772/60591

As the QD radius a increases (so that $a \gg a_{ex}^0$), the spherical interface of the two media (QD-matrix) passes to the plane <semiconductor material with the permittivity>-matrix interface. In this case, the exciton with the spatially separated electron and hole (the hole moves within the semiconductor material and the electron lies in the borosilicate glass matrix) becomes two-dimensional [20-22].

The primary contribution to the potential energy of the Hamiltonian (10) describing exciton motion in a nanosystem containing a large-radius QD, $a \gg a_{ex}^0$, is made by the electron-hole Coulomb interaction energy $V_{eh}(r)$ (11). The energy of the hole and electron interaction with self- $V_{hh'}(r_h, a, \varepsilon)$ (6), $V_{ee'}(r_h, a)$ (7) and "foreign" $V_{eh'}(\boldsymbol{r}_e, \boldsymbol{r}_h, a)$ (9), $V_{he'}(\boldsymbol{r}_e, \boldsymbol{r}_h, a)$ (8) images make a significantly smaller contribution to the potential energy of the Hamiltonian (10). In the first approximation, this contribution can be disregarded. In this case, only the electron-hole Coulomb interaction energy (11) remains in the potential energy of the Hamiltonian (10) [20-22]. The Schrodinger equation with such a Hamiltonian describes a two-dimensional exciton with a spatially separated electron and hole (the electron moves within the matrix, and the hole lies in the semiconductor material with the permittivity ε_2), the energy spectrum of which takes the following form [33, 34]:

$$E_n = -\frac{Ry_{ex}^0}{\left(n+1/2\right)^2}, \qquad Ry_{ex}^0 = \frac{\left(\varepsilon_1+\varepsilon_2\right)^2}{4\varepsilon_1^2\varepsilon_2^2}\left(\frac{\mu_0}{m_0}\right)Ry_0 \tag{13}$$

where n = 0, 1, 2... is the principal quantum number of the exciton and Ry_0 = 13.606 eV is the Rydberg constant. The Bohr radius of such a two-dimensional exciton is described by the following formula:

$$a^0{}_{ex} = \frac{2\varepsilon_1\varepsilon_2\hbar^2}{\varepsilon_1+\varepsilon_2\mu_0 e^2}, \tag{14}$$

and the binding energy of the ground state of such a two-dimensional exciton, according to (13), is written as:

$$E_{ex}^0 = -4Ry_{ex}^0 \tag{15}$$

The binding energy (15) of the exciton ground state is understood as the energy required for bound electron and hole state decay (in a state where n = 0).

To determine the ground-state energy of an exciton (with a spatially separated electron and hole) in a nanosystem containing QDs of the radius a, we applied the variational method. When choosing the variational exciton wave function, we used an approach similar to that developed in [14]. Let us write the variational radial wave function of the exciton ground-state (1s electron state and 1s hole state) in the nanosystem under study in the following form [20-22]:

$$\psi_0\left(\boldsymbol{r_e},\boldsymbol{r_h},r,a\right)=A\exp\left(-\frac{\mu(a)}{\mu_0}\frac{r}{a_{ex}^0}\right)\frac{\left(a^2-r_h^2\right)}{a^2}\times\frac{\left(r_e^2-a^2\right)}{a^2}\frac{r}{a}\frac{\left|\boldsymbol{r_e}-\left(a/r_h\right)^2\boldsymbol{r_h}\right|r_h}{a^2}\frac{\left|\boldsymbol{r_h}-\left(a/r_e\right)^2\boldsymbol{r_e}\right|r_e}{a^2} \tag{16}$$

Here, the coefficient A is determined from the condition of normalization of the exciton wave function (16):

$$\int_a^\infty r_e dr_e\int_0^a r_h dr_h\int_r^{r_e+r_h}\psi_0^2\left(\boldsymbol{r_e},\boldsymbol{r_h},r,a\right)rdr=1$$

and the effectively reduced exciton mass $\mu(a)$ is the variational parameter.

As the QD radius a increases (so that $a \gg a_{ex}^0$), a two-dimensional exciton is formed in the nanosystem. This leads to the variational exciton wave function (16) containing the Wannier-Mott two-dimensional exciton wave eigenfunction [33, 34]. Furthermore, the polynomials from r_e and r_h enter the exciton variational function (16), which make it possible to eliminate singularities in the functional $E_0(a,\mu(a))$ in the final analytical form.

To determine the exciton ground-state energy $E_0(a, \varepsilon)$ in the nanosystem under study using the variational method, we wrote the average value of the exciton Hamiltonian (10) in wave functions (16) as follows:

$$E_0\left(a,\mu(a)\right)=\psi_0\left(\boldsymbol{r_e},\boldsymbol{r_h},r,a\right)\left|H\left(\boldsymbol{r_e},\boldsymbol{r_h},r,a\right)\right|\psi_0\left(\boldsymbol{r_e},\boldsymbol{r_h},r,a\right)=$$
$$\int_a^\infty dr_e\int_0^a dr_h\int_r^{r_e+r_h}dr\,r\,r_e\,r_h\,\psi_0\left(\boldsymbol{r_e},\boldsymbol{r_h},r,a\right)H\left(\boldsymbol{r_e},\boldsymbol{r_h},r,a\right)\psi_0\left(\boldsymbol{r_e},\boldsymbol{r_h},r,a\right) \tag{17}$$

The dependence of the energy $E_0(a)$ of the exciton ground state ($n_e = 1$, $l_e = m_e = 0$; $n_h = 1$, $l_h = m_h = 0$) (n_e, l_e, m_e and n_h, l_h, m_h are the principal, orbital and magnetic quantum numbers of the electron and hole, respectively) on the QD radius, a is calculated by minimizing the functional $E_0(a, \mu(a))$ (17):

http://dx.doi.org/10.5772/60591

$$\frac{\partial E_0\left(a,\mu\left(a\right)\right)}{\partial\mu\left(a\right)} = F\left(\mu\left(a\right),a\right) \tag{18}$$

Without writing cumbersome expressions for the first derivative of the functional $\partial E_0(a, \mu(a))/\partial\mu(a) = F(\mu(a), a)$, we present the numerical solution to the equation $F(\mu(a), a) = 0$ (18) in tabulated form. This follows from the table that the solution to this equation is the function $\mu(a)$, which monotonically varies weakly within the limits [20-22]:

$$0.304 \le \mu\left(a\right) / m_0 \le 0.359 \tag{19}$$

as the QD radius a varies within the range

$$2.0 \le a \le 29.8 \text{ nm} \tag{20}$$

(m_0 is the electron mass in a vacuum). In this case, the reduced exciton effective mass $\mu(a)$ (19) in the nanosystem differs slightly from the effective mass of an exciton (with a spatially separated hole and electron) $\mu = 0.304m_0$ by the value $(\mu(a) - \mu_0)/\mu_0 \le 0.18$ when the QD radii vary within the range (20).

Simultaneously substituting the values of the variational parameter $\mu(a)$ (19) from Table 1 with the corresponding QD radii from the range (20) into the functional $E_0(a, \mu(a))$ (17), we obtain the exciton ground-state energy $E_0(a, \varepsilon)$ (17) as a function of the QD radius a [20-22].

a, nm	$\mu(a)/m_0$
2.0	0.359
3.0	0.352
4.0	0.345
5.0	0.338
6.0	0.331
8.0	0.325
10.0	0.319
15.0	0.313
20.0	0.308
29.8	0.304

Table 1. Variational parameter $\mu(a)$ as a function of the zinc selenide QD radius a.

The results of the variational calculation of the energy of the ground state of an exciton $E_0(a, \varepsilon)$ (17) in the nanosystem under study containing zinc selenide QDs of the radius a (20) are shown in the Figure 1 [20-22]. Here, the values of function $\mu(a)$ (19) and the results of the

variational calculation of the exciton ground-state energy $E_0(a, \varepsilon)$ (17) are obtained for a nanosystem containing zinc selenide QDs, synthesized in a borosilicate glass matrix, as studied in the experimental works [10, 19].

In the experimental work [10], borosilicate glass samples doped with zinc selenide with concentrations ranging from x = 0.003-1%, obtained by the sol-gel method, were studied. According to X-ray diffraction measurements, the average radii a of ZnSe QDs formed in the samples were within $a \approx$ 2.0-4.8 nm. In this case, the values of $\tilde{a}$ were comparable to the exciton Bohr radius $a_{ex} \approx$ 3.7 nm in a zinc selenide single crystal. At low QD concentrations (x = 0.003 and 0.06%), their interaction can be disregarded. The optical properties of such nanosystems are primarily controlled by the energy spectra of electrons and holes localized near the spherical surface of individual QDs synthesized in the borosilicate glass matrix.

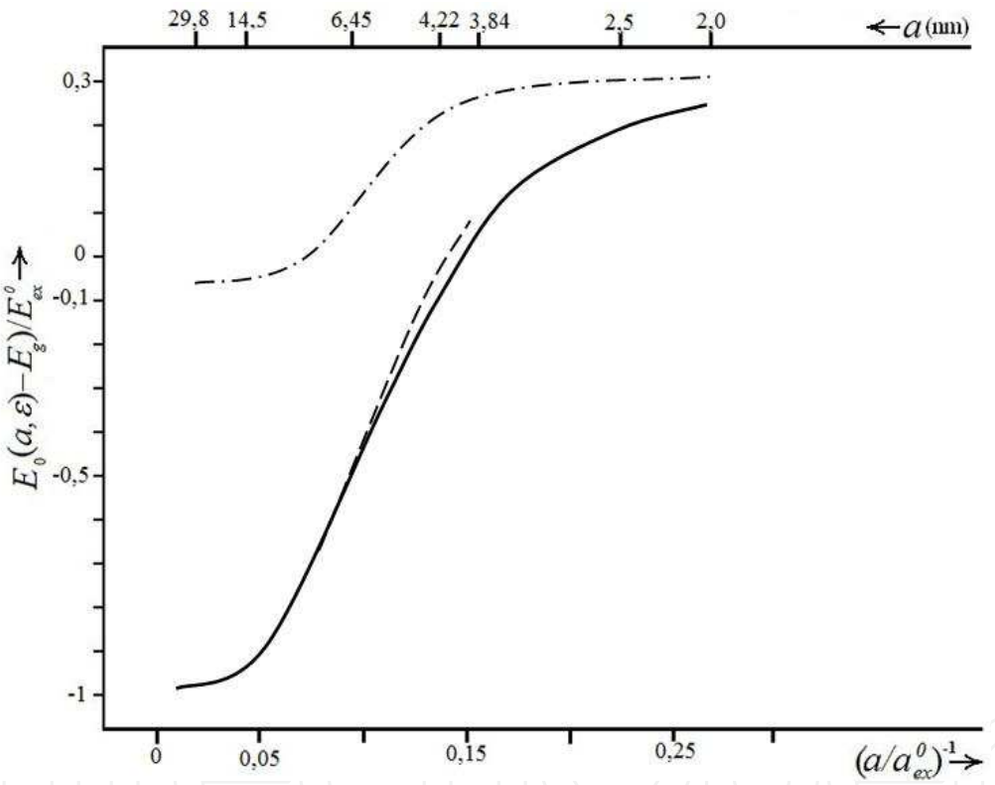

Figure 1. Dependences of the exciton ground state-energy ($E_0(a,\varepsilon) - E_g$) (17) (solid curve) and the binding energy of the exciton ground state ($E_{ex}(a, \varepsilon) - E_g$) (21) (dashed curve) on the zinc selenide QD radius a in the model of an exciton with a spatially separated electron and hole. The dash-dotted curve is the dependence of the exciton ground-state energy ($E_0(a, \varepsilon) - E_g$) on the zinc selenide QD radius a in the exciton model, in which the electron and hole move within the zinc selenide QD volume [16]. Eg = 2.823 eV is the band gap in a zinc selenide single crystal; E_{ex}^0 = 1.5296 eV (15) and a_{ex}^0, = 0.573 nm (14) are, respectively, the binding energy of the ground state and the Bohr radius of a two-dimensional exciton with a spatially separated electron and hole.

In [10, 19], a peak in the low-temperature luminescence spectrum at an energy of $E1 \approx$ 2.66 eV was observed at the temperature T = 4.5 K in samples with x = 0.06%; this energy is lower than the band gap of a zinc selenide single crystal (E_g = 2.823 eV). The shift of the peak of the low-

http://dx.doi.org/10.5772/60591

temperature luminescence spectrum with respect to the band gap of the ZnSe single crystal to the short-wavelength region is $\Delta E1 = (E1 - E_g) \approx -165$ meV. The authors of [10] assumed that the shift $\Delta E1$ was caused by quantum confinement of the energy spectra of electrons and holes localized near the spherical surface of individual QDs, and that it was associated with a decrease in the average radii a of zinc-selenide QDs at low concentrations ($x = 0.06\%$). In this case, the problem of the quantum confinement of which electron and hole states (the hole moving within the QD volume and the electron localized at the outer spherical QD-dielectric matrix interface or the electron and hole localized in the QD volume) caused such a shift of the luminescence-spectrum peak remained open.

Comparing the exciton ground-state energy $(E_0(a,\varepsilon) - E_g)$ (17) with the energy of the shift in the luminescence-spectrum peak $\Delta E1 \approx -165$ meV, we obtained the average zinc selenide QD radius $a1 \approx 4.22$ nm (see Figure 1) [20-22]. The QD radius $a1$ may be slightly overestimated, since the variational calculation of the exciton ground-state energy can yield slightly overestimated energies [33, 34]. The determined average QD radius $a1$ was found to be within the range of the average radii of zinc selenide QDs ($a \approx 2.0$-4.8 nm) studied under the experimental conditions of [10, 19].

It should be noted that the average Coulomb interaction energy $\overline{V}_{eh}(a, \varepsilon) = \psi_0(\boldsymbol{r_e}, \boldsymbol{r_h}, r, a) \mid V_{eh}(r) \mid \psi_0(\boldsymbol{r_e}, \boldsymbol{r_h}, r, a)$ between the electron and hole primarily contributed to the ground-state energy (17) of the exciton in the nanosystem containing zinc selenide QDs with radii $a1$ comparable to the exciton Bohr radius in a zinc-selenide single crystal ($a_{ex} \approx 3.7$ nm). In this case, the average energy of the interaction of the electron and hole with self- and "foreign" images,

$$\begin{aligned}&\left(\overline{V}_{ee'}(a,\varepsilon) + \overline{V}_{hh'}(a,\varepsilon) + \overline{V}_{eh'}(a,\varepsilon) + \overline{V}_{he'}(a,\varepsilon) \right) = \\ &= \langle \psi_0(r_e, r_h, r, a) \mid V_{ee'}(r_e, a, \varepsilon) + V_{hh'}(r_h, a, \varepsilon) + V_{eh'}(r_e, r_h, a, \varepsilon) + V_{he'}(r_e, r_h, a, \varepsilon) \mid \psi_0(r_e, r_h, r, a) \rangle\end{aligned}$$

yielded a significantly smaller contribution to the exciton ground-state energy (17),

$$0.04 \le \left| \left[V_{ee'}(a, \varepsilon) + V_{hh'}(a, \varepsilon) + V_{eh'}(a, \varepsilon) + V_{he'}(a, \varepsilon) \right] / E_0(a, \varepsilon) \right| \le 0.12 \left[20 - 22 \right].$$

Thus, the short-wavelength shift $\Delta E1$ of the low temperature luminescence spectrum peak is caused by renormalization of the electron-hole Coulomb interaction energy $V_{eh}(r)$ (11), as well as renormalization of the energy $U(r_e, r_h, r, a, \varepsilon)$ (5) of the polarization interaction of the electron and hole with the spherical QD-dielectric matrix interface, which is associated with spatial confinement of the quantization region by the QD volume. In this case, the hole moves within the QD volume and the electron is localized at the outer spherical QD-dielectric matrix interface.

The binding energy of the ground state of an exciton (with a spatially separated electron and hole) $E_{ex}(a, \varepsilon)$ in a nanosystem containing zinc selenide QDs of the radius a is the solution to

the radial Schrodinger equation with a Hamiltonian containing, in contrast to Hamiltonian (10), only the terms $V_{he'}(r_e, r_h, a, \varepsilon)$ (8) and $V_{eh'}(r_e, r_h, a, \varepsilon)$ (9) in the polarization interaction energy $U(\mathbf{r}_e, \mathbf{r}_h, a, \varepsilon)$ (5), which describe the energies of the hole and electron interaction with "foreign" images, respectively [15, 27, 28]. Therefore, the exciton ground-state binding energy $Eex(a, \varepsilon)$ is defined by the expression [20-22]:

$$E_{ex}\left(a,\varepsilon\right) = E_0\left(a,\varepsilon\right) - \left\langle \psi_{\rm o}\left(r_e, r_h, r, a\right) \middle| \left(V_{hh'}\left(r_h, a, \varepsilon\right) + V_{ee'}\left(r_e, a, \varepsilon\right)\right) \middle| \psi_{\rm o}\left(r_e, r_h, r, a\right) \right\rangle, \tag{21}$$

where the term $\langle \psi_o(r_e, r_h, r, a) | \left(V_{h\,h'}(r_h, a, \varepsilon) + V_{ee'}(r_e, a, \varepsilon)\right) | \psi_o(r_e, r_h, r, a) \rangle$ describes the average energy of hole and electron interaction with self-images.

Since the average energies of the interaction of the hole with its image and the average energies of the interaction of the electron with its image deliver contributions that take opposing signs to expression (21), they significantly compensate for each other. Therefore, the binding energies of the exciton ground state $E_{ex}(a, \varepsilon)$ (21) slightly differs from the corresponding total energies of the exciton ground state $E_0(a, \varepsilon)$ (17). This difference,

$$\Delta = \left| \left(\; E_{ex}\left(a,\varepsilon\right) - E_0\left(a,\varepsilon\right) \; \right) / \, E_{ex}\left(a,\varepsilon\right) \right|,$$

varies within $\Delta \le 4\%$, as QD radii a varies within the range $3.84 \le a \le 8.2$ nm (see Figure 1) [20-22].

Figure 1 shows the dependences of the total energy $E_0(a, \varepsilon)$ (17) and the binding energy $E_{ex}(a, \varepsilon)$ (21) of the ground state of the exciton with a spatially separated electron and hole on the QD size for a nanosystem containing zinc selenide QDs of the radius a. We can see that the bound states of electron-hole pairs arise near the spherical surface of the QD, starting from the QD critical radius $a \ge a_c^{(1)} \approx 3.84$ nm. In this case, the hole is localized near the QD inner surface and the electron is localized at the outer spherical QD-dielectric matrix interface. Starting from the QD radius $a \ge a_c^{(1)}$, the electron-hole pair states are in the region of negative energies (counted from the top of the band gap E_g for a zinc selenide single crystal), which corresponds to the electron-hole bound state [20-22, 29-23]. In this case, the electron-hole Coulomb interaction energy $V_{eh}(r)$ (11) and the energy $U(r_e, r_h, r, a, \varepsilon)$ (5) of the polarization interaction of the electron and hole with the spherical QD-dielectric matrix interface dominate the energy of the quantum confinement of the electron and hole in the nanosystem under study.

The total energy $|E_0(a, \varepsilon)|$ (17) and the binding energy $|E_{ex}(a, \varepsilon)|$ (21) of the ground state of the exciton with a spatially separated electron and hole increases with QD radius a. In the range of radii

$$4.0 \le a \le 2.8\,\text{nm} \tag{22}$$

the binding energy $|E_{ex}(a, \varepsilon)|$ (21) of the exciton ground state significantly (by a factor of 4.1-76.2) exceeds the exciton binding energy in a zinc selenide single crystal, $E_{ex}^0 \approx -21.07$ meV. Starting from the QD radius $a \geq a_c^{(2)} \approx 29.8$ nm, the total energies (17) and binding energies (21) of the exciton ground state asymptotically tend to the value $E_{ex}^0 = -1.5296$ eV, which characterizes the binding energy of the ground state of a two-dimensional exciton with a spatially separated electron and hole (see the figure 1) [20-22, 29-32].

The obtained values of the total energy $E_0(a, \varepsilon)$ (17) of the exciton ground state in the nanosystem satisfy the inequality

$$\left(E_0\left(a,\varepsilon\right) - E_g\right) \ll \Delta V(a) \tag{23}$$

where $\Delta V(a)$ is the potential-well depth for the QD electron. For a large class of II-VI semiconductors in the region of QD sizes, $a \geq a_{ex}^0$, $\Delta V(a) = 2.3\text{-}2.5$ eV [7]. Satisfaction of condition (23) likely makes it possible to disregard the effect of the complex structure of the QD valence band on the total energy (17) and the binding energy (21) of the exciton ground state in the nanosystem under study when deriving these quantities.

The effect of a significant increase in the binding energy $|E_{ex}(a, \varepsilon)|$ (21) of the exciton ground state in the nanosystem under study, according to formulas (5) to (9), (11), (13) to (15), (17) and (21) is controlled by two factors [20-22, 29-32]: (i) a significant increase in the energy of the electron-hole Coulomb interaction $|V_{eh}(r)|$ (11) and an increase in the energy of the interaction of the electron and hole with "foreign" images $|V_{eh'}(r_e, r_h, r, a, \varepsilon)|$ (9), $|V_{he'}(r_e, r_h, r, a, \varepsilon)|$ (8) (the "dielectric enhancement" effect [34]); (ii) spatial confinement of the quantization region by the QD volume. In this case, as the QD radius a increases, starting from $a \geq a_c^{(2)} \approx 52\ a_{ex}^0 \approx 29.8$ nm, the exciton becomes two-dimensional, with a ground-state energy of E_{ex}^0 (15), which exceeds the exciton binding energy E_{ex} in the zinc selenide single crystal by almost two orders of magnitude:

$$\left(\left|E_{ex}^0 / \overline{E_{ex}^0}\right| \approx 72.6\right).$$

The "dielectric enhancement" effect is caused by the following factor. When the matrix permittivity ε_1 is significantly smaller than the QD permittivity ε_2, the most important role in the electron-hole interaction in the nanosystem under study is fulfilled by the field induced by these quasiparticles in the matrix. In this case, electron-hole interaction in the nanosystem appears to be significantly stronger than in an infinite semiconductor with the permittivity ε_2 [34].

In [16], in the nanosystem experimentally studied in [10], an exciton model in which the electron and hole move within the zinc selenide QD volume was studied. Using the variational method, within the modified effective mass method, the dependence of the exciton ground-

state energy $E_0(a, \varepsilon)$ on the QD radius a in the range (20) was obtained in [16] (see Figure 1). It was shown that, as the QD radius increased, starting from $a \geq a_c = 3.90\ a_{ex}^0 = 1.45$ nm, a bulk exciton appeared in the QD; its binding energy,

$$\overline{E_{ex}^0} = -\frac{\hbar^2}{2\mu\left(\overline{a_{ex}^0}\right)^2} \tag{24}$$

was 21.07 meV ($\mu = 0.132m_0$ and $\overline{a_{ex}^0} = 3.7$ nm are the reduced effective mass and Bohr radius of the exciton in the zinc-selenide forming the QD volume). The bulk exciton in the QD is understood as an exciton whose structure (reduced mass, Bohr radius and binding energy) in the QD does not differ from the structure of an exciton in an infinite semiconductor material. As the QD radius a increases ($a \geq a_c$), the exciton ground-state energy $E_0(a)$ asymptotically follows the binding energy of the bulk exciton (24) (see Figure 1) [20-22, 29-32].

Thus, using the exciton model, in which an electron and hole move in the QD volume, it is impossible to interpret the mechanism of the appearance of the nanosystem luminescence-spectrum peak with the shift $\Delta E1 \approx -165$ meV, obtained in [10, 19].

A comparison of the dependences of the exciton ground-state energy $E_0(a)$ in the nanosystem [10], obtained using two-exciton models (see Figure 1) (the electron and hole move within the zinc selenide QD volume [16]) (model **I**); the hole moves within the zinc selenide QD volume and the electron is localized in the boron silicate glass matrix near the QD spherical surface (model **II**), allowing for the following conclusion. In model **I**, as the QD radius a increases, starting from $a \geq a_c \approx 14.5$ nm, the exciton ground- state energy $E_0(a)$ asymptotically follows the binding energy of the bulk exciton $\overline{E_{ex}^0} \approx -21.07$ meV (24). In model II, as the QD radius increases, starting from $a \geq \quad a_c^{(2)} \approx 29.8$ nm, the exciton ground-state energy (17) asymptotically follows $E_{ex}^0 = -1.5296$ eV (15) (characterizing the binding energy of the ground state of a two- dimensional exciton with a spatially separated electron and hole), which is significantly lower than $\overline{E_{ex}^0} \approx -21.07$ meV [20-22, 29-32].

3. Excitonic quasimolecules formed from spatially separated electrons and holes

We considered a model nanosystem [23, 24] that consisted of two spherical semiconductor QDs, A and B, synthesized in a borosilicate glass matrix with the permittivity ε_1. Let the QD radii be a and the spacing between the spherical QD surfaces be D. Each QD is formed from a semiconductor material with the permittivity ε_2. For simplicity, without loss of generality, we assumed that holes h (A) and h (B) with the effective masses m_h were in the QD (A) and QD (B) centres and the electrons $e(1)$ and $e(2)$ with the effective masses $m_e^{(1)}$ were localized near the

spherical QD(A) and QD (B) surfaces, respectively. The above assumption was reasonable, since the ratio between the effective masses of the electron and hole in the nanosystem was much smaller that unity: $\left(\left(m_e^{(1)}/m_h\right)\ll 1\right)$. Let us assume that there was an infinitely high potential barrier at the spherical QD-matrix interface. Therefore, in the nanosystem, holes did not leave the QD bulk and electrons did not penetrate into the QDs.

In the context of the adiabatic approximation and effective mass approximation, using the variational method, we obtained the total energy $E_0(\widetilde{D},\,\tilde{a})$ and the binding energy $E_e(\widetilde{D},\,\tilde{a})$ of the biexciton singlet ground state (the spinning of the electrons $e(1)$ and $e(2)$ were antiparallel) in such a system as functions of the spacing between the QD surfaces D and the QD radius a [23, 24]:

$$E_0\left(\tilde{D},\tilde{a}\right)=2E_{\hat{a}x}\left(\tilde{a}\right)+E\left(\tilde{D},\tilde{a}\right), \tag{25}$$

Here, the binding energy $E_{ex}(\tilde{a})$ (17) of the ground state of the exciton (formed from an electron and a hole spatially separated from the electron) localized above the QD(A) (or QD(B)) surface was determined in [23, 24] (by the parameters $\tilde{a}=\left(a/a_{ex}^0\right)$ ($a_{ex}^0=$ 3.7 nm and the exciton Bohr radius in a single crystal ZnSe, $\widetilde{D}=\left(D/a_{ex}^0\right)$). For the nanosystem under study, the values of the binding energies $E_{ex}(\tilde{a})$ were calculated in [23, 24] for use in the experimental conditions of [10, 19].

The results of the variational calculation of the binding energy $E_{\text{в}}(\widetilde{D},\,\tilde{a})$ of the biexciton singlet ground state in the nanosystem of ZnSe and QDs with an average radii of $\bar{a}_1$=3.88 nm,, synthesized in a borosilicate glass matrix, are shown in [23, 24]. Such a nanosystem was experimentally studied in [10, 19]. In [10, 19], the borosilicate glassy samples doped with ZnSe to the content x from x = 0.003-1% were produced using the sol-gel technique. At a QD content of x = 0.06 %, one must take into account the interaction of charge carriers localized above the QD surfaces.

The binding energy $E_{\text{в}}(\widetilde{D},\,\tilde{a})$ of the biexciton singlet ground state in the nanosystem of ZnSe QDs with average radii of $\bar{a}_1$=3.88 nm has a minimum of $E_{\text{в}}^{(1)}(D_1,\ \bar{a}_1)\approx -4,2$ meV (at the spacing $D_1\cong 3.2$ nm) [23, 24]. The value of $E_{\text{в}}^{(1)}$ corresponds to the temperature $T_c\approx 49\ K$. In [23, 24], it follows that a biexciton (excitonic quasimolecule) is formed in the nanosystem, starting from a spacing between the QD surfaces of $D\geq D_c^{(1)}\cong 2,4\ \ nm$. The formation of such a excitonic quasimolecule (biexciton) is of the threshold character and possible only in a nanosystem with QDs with average radii $\bar{a}_1$, such that the spacing between the QD surfaces D exceeds a certain critical spacing $D_c^{(1)}$. Moreover, the exciton quasimolecule (biexciton) can exist only at temperatures below a certain critical temperature, i.e., $T_c\approx 49$ K [23, 24].

As follows from the results of variational calculation [23, 24], the binding energy of an exciton (formed from an electron and a hole spatially separated from the electron) localized above the surface of the QD(A) (or a QD(B)) with an average radius of $\bar{a}_1$=3, 88 nm is

$E_{ex}(\tilde{a}_1) \cong -54$ meV . In this case, the energy of the biexciton singlet ground state $E_0(\widetilde{D}, \tilde{a})$ (25) takes the value $E_0(\widetilde{D}, \tilde{a})$ = -112meV.

From the results of variational calculation [23, 24], of the biexciton (exciton quasimolecule) binding energy $E_e(\widetilde{D}, \tilde{a})$, it follows that the major contribution to the binding energy (25) is made by the average energy of the exchange interaction of the electrons $e(1)$ and $e(2)$ alongside holes h (A) and h (B). At the same time, the energy of the Coulomb interaction makes a much smaller contribution of the biexciton binding energy $E_e(\widetilde{D}, \tilde{a})$ (25).

The major contribution to the exchange is interaction energy, created by the energy of the exchange interaction of the electron $e(1)$ with the holes h (B), as well as of the electron $e(2)$ with the holes h (B), and of the electron $e(2)$ with the holes h (A). The major contribution to the Coulomb is interaction energy, created by the energy of the Coulomb interaction of the electron $e(1)$ with the holes h (B), as well as of the electron $e(2)$ with the holes h (A) [23, 24].

As the spacing D between the QD(A) and QD(B) surfaces is increased, starting from $D \geq D_c^{(2)} \cong 16,4$ nm, the average Coulomb interaction energy substantially decreases. In addition, because of the decrease in the overlapping of the electron wave function, the average exchange interaction energy also substantially decreases. Consequently, the average Coulomb interaction energy and the average energy of the exchange interaction of the electrons $e(1)$ and $e(2)$ with the holes h (A) and h (B) sharply decrease in comparison with the exciton binding energy $E_{ex}(\tilde{a})$ (17) [23, 24], resulting in decomposition of the biexciton in the nanosystem into two excitons (formed of spatially separated electrons and holes) localized above the QD(A) and QD(B) surfaces.

4. Theory of new superatoms — Analogue atoms from the group of alkali metals

The idea of superatoms (or artificial atoms) is essential for the development of mesoscopic physics and chemistry [20-22, 29, 30]. Superatoms are nanosized quasi-atomic nanostructures formed from spatially separated electrons and holes (the hole in the volume of the QD and the electron is localized on the outer spherical quantum dot matrix dielectric interface) [20-22, 29, 30]. This terminology can be accepted as correct, given the similarities between the spectra of discrete electronic states of atoms and superatomic atoms, and the similarities in terms of their chemical activities [20-22, 29, 30].

In [20-22], within the framework of the modified effective mass method [14], the theory of artificial atoms formed from spatially separated electrons and holes (holes moving in the volume of a semiconductor (dielectric) QD and an electron localized on the outer spherical interface between the QD and a dielectric matrix) is developed. The energy spectrum of superatoms (excitons of spatially separated electrons and holes) from QD radius $a \geq ac$ (about 4 nm) is fully discrete [20-22, 29, 30]. This is referred to as a hydrogen-superatom and is localized on the surface of a valence electron QD. The energy spectrum of the superatom

consists of a quantum-dimension of discrete energy levels in the band gap of the dielectric matrix. Electrons in superatoms are localized in the vicinity of the nucleus (QD). The electrons move in well-defined atomic orbitals and serve as the nucleus of QD, containing in its volume semiconductors and insulators. Ionization energy superatoms take on large values (of the order of 2.5 eV), which is almost three orders of magnitude higher than the binding energy of the excitons in semiconductors [20-22, 29, 30].

We will briefly discuss the possible physical and chemical effects that are relevant for the results of this paper. In our proposed [20-22, 29, 30] model of a hydrogen superatom localized on the surface of the QD is a valence electron. In quasi-atomic structures of the outer valence, electrons can participate in a variety of physical and chemical processes, similar to the atomic valence electrons in atomic structures. Artificial atoms have the ability to connect to the electron orbitals of electrons N (where N can vary from one to several tens). At the same time, the number of electrons N can take values of the order of a few tens or even surpass the serial numbers of all the known elements found in Mendeleev's table [20-22, 29, 30]. This new effect allows for attaching to the electronic orbitals of artificial atoms N electrons, causing a high reactivity and opening up new possibilities for superatoms related to their strong oxidizing properties, increasing the possibility of substantial intensity in photochemical reactions during catalysis and adsorption, as well as their ability to form many new compounds with unique properties (in particular, the quasi-molecule and quasicrystals) [24, 29, 30]. Therefore, studies aimed at the theoretical prediction of the possible existence of artificial new atoms (not listed in the Mendeleev table) and to their study in terms of experimental conditions are very relevant.

Quantum discrete states of the individual atoms of alkali metals are determined by the movement of only one, i.e., the outermost valence electron, around a symmetric atomic core (containing the nucleus and the remaining electrons) [35]. In the hydrogen superatom formed quantum-energy spectra of discrete energy levels of the valence electron [20-22, 29, 30]. Thus, the observed similarity of the spectra of discrete electronic states and individual superatoms alkali metal atoms, as well as the similarity of their chemical activity [20-22, 29, 30, 35].

In Section 4, on the basis of a spectroscopic analogy of electronic states of artificial atoms and individual alkali metal atoms, a new artificial atom is theoretically predicted, which is similar to the new alkali metal atom.

In [20-22, 29, 30], a new model of an superatom is proposed, which is a quasi-zero-dimensional nanosystem consisting of a spherical QD (nucleus superatom) with radius a and which is included within its scope as a semiconductor (dielectric) with a dielectric constant ε_2, surrounded by a dielectric matrix with a dielectric constant ε_1. A hole h with the effective mass m_h moves in the QD volume, while an electron e with the effective mass $m_e^{(1)}$ lies in the dielectric matrix. In such a nanostructure, the lowest electronic level is situated in the matrix and the humble hole level is the volume QD. Large shift of the valence band (about 700 meV) is the localization of holes in the volume QD. A large shift of the conduction band (about 400 meV) is a potential barrier for electrons (electrons move in the matrix and do not penetrate into the volume QD). The Coulomb interaction energy of an electron and a hole, and the energy of the electron polarization interaction with the surface section (QD-matrix) (since the permittivity

ε_2 is far superior to QD permittivity ε_1 matrix) cause localization of the electron in the potential well above the surface of QD [20-22, 29, 30].

With increasing radius a QD, so that $a >> a_{ex}^0$ (where a_{ex}^0 (14) two-dimensional Bohr radius of the electron) spherical surface section (QD- matrix) transforms into a flat surface section. In this artificial atom, electrons localized on the surface (QD-matrix) become two-dimensional. In this case, the potential energy in the Hamiltonian describing the motion of an electron in a superatom, the main contribution to the energy of the Coulomb interaction $V_{eh}(r)$ (11) between an electron and a hole [20-22]. Polarization interaction energy of the electron and the hole with a spherical surface section (QD-matrix) delivers a much smaller contribution to the potential energy of the Hamiltonian and thus, contributions to a first approximation can be neglected [20-22]. In this regard, the two-dimensional electron energy spectrum En in the artificial atom takes the form (13).

Depending on the binding energy $E_{ex}(a,\varepsilon)$ of an electron in the ground state superatom (QD containing zinc-selenide radius a and surrounded by a matrix of borosilicate glass [10]) as obtained in [20-22] by the variational method, it follows that the bound state of an electron occurs near the spherical interface (QD-matrix), starting with the value of the critical radius QD $a \geq a_c^{(1)} = 3.84$ nm, when this hole moves in the volume QD and the electron is localized on the surface of the spherical section (QD-matrix). In this case, the Coulomb interaction energy $V_{eh}(r)$ (11) between the electron and the hole, and the energy of the polarization interaction of electrons and holes with a spherical surface section (QD-matrix) prevail over the size quantization of the energy of electrons and holes in the artificial atom. Thus, [20-22] found that the occurrence of superatoms had a threshold and was only possible if the radius of QD KT $a \geq a_c^{(1)} = 3.84$ nm.

With the increasing radius of a QD scan, an increase in the binding energy of the electron in the ground state superatom was observed. In the range of radii $4.0 \leq a \leq 29.8$ nm, the binding energy of the electron in the ground state superatom significantly exceeded (in (4,1-76,2) times) the value of the exciton binding energy $\tilde{E}^0_{ex} \approx 21.07$ meV in a single crystal of zinc-selenide [20-22]. Beginning with a radius QD $a \geq a_c^{(2)} = 29.8$ nm, the energy of the ground state of an electron in a superatom asymptotically follow the value $E^0_{ex} = -1.5296$ eV, which characterized the energy of the ground state of two-dimensional electrons in an artificial atom (15) [20-22].

The effect of significantly increasing the energy of the ground state of an electron in a superatom was primarily determined by two factors [20-22]: 1) a significant increase in the Coulomb interaction energy $|V_{eh}(r)|$ (2) electron-hole (the "dielectric enhancement" [34]); 2) the spatial limitations on the quantization volume QD, while with an increasing radius of a QD, since the radius of QD $a \geq a_c^{(2)} = 52a^0_{ex} = 29.8$ nm, superatoms became two-dimensional with a binding energy of the ground state E^0_{ex} (15), the value of which exceeded the exciton binding energy in a single crystal of zinc-selenide by two orders. The effect of "dielectric enhancement" as a result of the dielectric constant ε_1 of the matrix was much lower than the dielectric constant of QD ε_2, which played an essential role in the interaction between the electron and the hole in the superatom playing field produced by these quasi-particles in a matrix. Thus, the interaction between the electron and the hole in the superatom was significantly larger than in a semiconductor permittivity ε_2 [34].

Quantum discrete states of the individual atoms of alkali metals were determined by the movement of only one, the outermost valence electron, around a symmetric atomic core (containing the nucleus and the remaining electrons) [35]. Where large distances were the case between r electron and the nucleus (so that $r >> a0$, where $a0 = 0.053$ nm – the Bohr radius of the electron in a hydrogen atom), the field of the atomic core was described by the Coulomb field [35]:

$$V(r) = -\left(Ze^2 / r\right), \tag{26}$$

determining the interaction of the valence electron with the atomic core (Z – serial number of the atom in the periodic table of Mendeleev). The energy spectrum of a single atom of an alkali metal hydrogen-described spectrum [35] is given as follows:

$$E_{n^*} = -\frac{Ry^*}{\left(n^*\right)^2},\ Ry^* = Z^2\ Ry_0 \tag{27}$$

where $n^* = (n + y)$ and effective quantum number ($n = 1, 2, 3,...$ the principal quantum number); the amendment y depended on the orbital quantum number l. Amendments to y were due to the fact that the valence electron moved in the Coulomb field of the atomic core, where the nuclear charge was screened by core electrons. Amendment y corrections were determined by comparing the spectrum of (6) with its experimental values. The value of $y < 0$ and was numerically closer to the atomic core suitable valence electron orbit. The number of possible orbits of the valence electron in a single alkali metal atom such as a hydrogen atom, and [35].

The similarity of the individual series of neutral alkali metal atoms with the hydrogen Balmer series suggests that the energy spectra of neutral alkali metal atoms can be labelled valence electron radiation in transition from higher levels to the level of principal quantum number $n = 2$ [35].

In a single atom of an alkali metal valence electron moving in the Coulomb field of the atomic core (26) having the same functional dependence on r as the Coulomb field (11), in which the valence electron in hydrogen-like model of artificial atom. This leads to the fact that the energy spectra of the valence electron in a single atom of an alkali metal (27) and in the artificial atom (13) describe the spectrum of hydrogen-type. At the same time, the number of possible quantum states of valence electrons in a hydrogen-like artificial atom model is the same as the number of quantum states of discrete valence electrons in a single atom of an alkali metal [20-22, 29, 30].

Table 2 shows the position of the valence electron energy levels in the atoms of alkali metals (K, Rb, Sc) [35] and the new artificial atom X, as well as the level shifts of the valence electron (ΔE_{Rb}^{K}, ΔE_{Sc}^{Rb}, ΔE_{x}^{Sc}) relative to the adjacent level. Assume that the shift of the energy level E_x artificial atom X (relative to the energy level E_{sc} of the atom Sc) will be the same as the shift of the energy level E_{Rb} of the atom Rb (relative energy level E_{sc} of the atom Sc), (i.e., ΔE_{x}^{Sc} =

ΔE_{Sc}^{Rb}). In this case, the level of the valence electron artificial atom will be Ex = –593 meV. Using the dependence of the binding energy $E_{ex}(a,\varepsilon)$ of the ground state of an electron in an artificial atom [20-22] (QD containing zinc-selenide radius a and surrounded by a matrix of borosilicate glass [10]), we found the radius QD zinc-selenide $a1$ = 5.4 nm, which corresponded to the Ex = – 593 meV. It should be noted that the energy levels of a valence electron in the individual atoms of alkali metals (K, Rb, Sc) [35] and the new artificial atom X are located in the infrared spectrum.

Alkali metal atoms selected	Valence electron energy levels (meV)	Level shifts of the valence electron (meV)
K	- 7 21.1	
Rb	- 7 11.2	1 0
Sc	- 652	5 9
X	- 5 93	5 9

Table 2. Position of energy levels of the valence electron in some alkali metal atoms (K, Rb, Sc) and a new artificial atom, X. Level shifts of the valence electron (ΔE_{Rb}^{κ}, ΔE_{Sc}^{Rb}, ΔE_{x}^{Sc}) are relative to the adjacent level.

Thus, we propose a new model of an artificial atom that is a quasi-atomic heterostructure consisting of a spherical QD (nucleus superatom) radius a and which contains in its scope, zinc-selenide, surrounded by a matrix of borosilicate glass (in volume QD, h hole effectively moves mass m_h, e and the electron effective mass $m_e^{(1)}$ is located in the matrix), thus allowing for finding a new artificial atom X (absent in the Mendeleev periodic system), which is similar to a new single alkali metal atom. This new artificial atom of a valence electron can participate in various physical [20-22, 29, 30] and chemical [30, 35] processes that are analogous to atomic valence electrons in atomic systems (in particular, the selected alkali metal atoms [35]). Such processes are unique as a result of the new properties of artificial atoms: strong oxidizing properties that increases the possibility of substantial intensity in photochemical reactions during catalysis and adsorption, as well as their ability to form a plurality of the novel compounds with unique properties (in particular, the quasi-molecule and the quasicrystals [23, 24]).

The application of semiconductor nanoheterostructures as the active region nanolasers prevents small exciton binding energy in QD. Therefore, studies aimed at finding nanoheterostructures, which will yield a significant increase in the binding energy of the local electronic states in QDs, are relevant [20-22]. The effect of significantly increasing the energy of the electron in a hydrogen superatom [20-22, 29, 30] allows for better experimental detection of the existence of such superatoms at room temperatures and will stimulate experimental studies of nanoheterostructures containing superatoms, which can be used as active region nanolasers when working with optical transitions.

http://dx.doi.org/10.5772/60591

5. Conclusions

The theory of an exciton with a spatially separated electron and hole was developed within the framework of the modified effective mass method [14], in which the reduced effective exciton mass is a function of the semiconductor QD radius a. The average zinc-selenide QD radius was determined by comparing the dependence of the exciton ground-state energy (17) on the QD radius, obtained by the variational method within the modified effective mass method [14] and using the experimental peak of the low-temperature luminescence spectrum [10, 19]. It was shown that the short-wavelength shift of the peak of the low-temperature luminescence spectrum of the samples containing zinc selenide QDs, which was observed under the experimental conditions noted in [10, 19], was caused by renormalization of the electron-hole Coulomb interaction energy (11), as well as the energy created by the polarization interaction (5) of the electron and hole with the spherical QD-dielectric matrix interface, related to spatial confinement of the quantization region by the QD volume. In this case, the hole moves in the QD volume and the electron is localized at the outer spherical QD-dielectric matrix interface [20-22, 29-32].

To apply semiconductor nanosystems containing zinc-selenide QDs as the active region of lasers, it is required that the exciton binding energy $|E_{ex}(a, \varepsilon)|$ (21) in the nanosystem be at the order of several kT_0 and at room temperature T_0 (k is the Boltzmann constant) [13]. Nanosystems consisting of zinc-selenide QDs grown in a borosilicate glass matrix can be used as the active region of semiconductor QD lasers. In the range of zinc selenide QD radii a (22), the parameter $|E_{ex}(a, \varepsilon)/kT_0|$ take on significant values ranging from 3.1 to 56 [20-22, 29-32].

The effect of significantly increasing the binding energy (21) of the exciton ground state in a nanosystem containing zinc selenide QDs with radii a (22) was detected; compared to the exciton binding energy in a zinc selenide single crystal, the increase factor was 4.1-72.6. [20-22, 29-32]. It was shown that the effect of significantly increasing the binding energy (21) of the exciton ground state in the nanosystem under study was controlled by two factors [20-22, 29-32]: (i) a substantial increase in the electron-hole Coulomb interaction energy (11) and an increase in the energy of the interaction of the electron and hole with "foreign" images (8), (9) (the "dielectric enhancement" effect [34]); (ii) spatial confinement of the quantization region by the QD volume; in this case, as the QD radius a increased, starting from $a \geq a_c^{(2)} \approx 29.8$ nm, the exciton became two-dimensional with a ground-state energy (15), which exceeded the exciton binding energy in a zinc selenide single crystal by almost two orders of magnitude.

A review devoted to the theory of excitonic quasimolecules (biexciton) (made up of spatially separated electrons and holes) in a nanosystem that consists of ZnSe QDs synthesized in a borosilicate glass matrix was developed within the context of the modified effective mass approximation. Using the variational method, we obtained the total energy and the binding energy of the biexciton singlet ground state in such a system as functions of the spacing between the QD surfaces and the QD radius. It was established that, in a nanosystem composed of ZnSe QDs with the average radii $\bar{a}_1$, the formation of a biexciton (exciton quasimolecule) was of the threshold character and possible in a nanosystem where the spacing D between the

QD surfaces is defined by the condition $D_c^{(1)} \le D \le D_c^{(2)}$ [23, 24]. Moreover, the exciton quasimolecule (biexciton) can exist only at temperatures below a certain critical temperature, i.e., $T_c \approx 49$ K [23, 24]. It was established that the spectral shift of the low temperature luminescence peak [10, 19] in such a nanosystem resulted due to quantum confinement of the energy of the biexciton singlet ground state.

Thus, we propose a new model of an artificial atom, which is a quasi-atomic heterostructure consisting of a spherical QD (nucleus superatom) with radius a and which contains in its scope zinc selenide, surrounded by a matrix of borosilicate glass (in volume QD moves h hole effective mass m_h, e and the electron effective mass $m_e^{(1)}$ is located in the matrix), and which is allowed to find a new artificial atom X (absent in the Mendeleev periodic system), which is similar to a new single alkali metal atom. This new artificial atom of valence electron can participate in various physical [20-22, 29, 30] and chemical [30, 35] processes that are analogous to atomic valence electrons in atomic systems (in particular, the selected alkali metal atoms [35]). Such processes are unique due to the new properties of artificial atoms: strong oxidizing properties that increase the possibility of substantial intensity in photochemical reactions during catalysis and adsorption, as well as their ability to form plurality among novel compounds with unique properties (in particular, the quasi-molecule and the quasicrystals [23, 24]).

Author details

Sergey I. Pokutnyi[1*] and Włodzimierz Salejda[1*]

*Address all correspondence to: Pokutnyi_Sergey@inbox.ru; Wlodzimierz.Salejda@pwr.edu.pl

1 Chuiko Institute of Surface Chemistry, National Academy of Sciences of Ukraine, Kyiv, Ukraine

2 Technical University of Wroclaw, Wroclaw, Poland

References

[1] Ekimov, A., Onushchenko, A., (1981). Size quantization of electrons in microcrystals. *Journal Experimental Theoretical Physics Letters*. 34, 345-348.

[2] Ekimov, A., Onushchenko, A., (1984). Size quantization of electrons in semiconductor microcrystals. *Journal Experimental Theoretical Physics Letters*. 40, 1136-1139.

[3] Ekimov, A., Efros, A., (1985). Excitons in semiconductor microcrystals. *Solid State Communication.* 56, 921-924.

[4] Ekimov, A., Onushchenko, A., Efros, A., (1986). Size quantization of electron-hole pairs in nanocrystals. *Journal Experimental Theoretical Physics Letters*. 43, 376-379.

[5] Chepik, D., Efros, A., Ekimov, A., (1990). Spectroscopy of excitons in semiconductor nanocrystals. *Journal of Luminescence.* 47, 113-118.

[6] Ekimov, A., Hache, F., Schanne-Klein, M., (2003). Optical properties semiconductor quantum dots. *Journal Optical Society American*. B 20, 100 -108.

[7] Grabovskis, V., Dzenis, Y., Ekimov, A., (1989). Photoluminescences of excitons in semiconductor nanocrystals. *Physics Solid State*. 31, 149 -152.

[8] Alferov, J.I., (2002). Progress development in semiconductor nanostructures. *Physics Uspekhi*. 172, 1068 - 1074.

[9] Alferov, J.I., (1998). Optical properties in semiconductor nanostructures. *Semiconductors.* 32, 1-8.

[10] Bondar, V.N., Brodin, M.S., (2010). Optical properties semiconductor quantum dots. *Semiconductors.* 44, 884-890.

[11] Efros, A.L., Efros, Al. L., Interband absorption light in semiconductor sphere. (1982). *Sov. Phys. Semiconductors*. 16, 955- 962.

[12] Pokutnyi, S.I., (2004). Size quantization Stark effect in semiconductor quantum dots. *J. Appl. Phys*. 96, 1115-1122.

[13] Pokutnyi, S.I., (2005). Optical nanolaser heavy hole transitions in quasi-zero- dimensional semiconductors nanosystems. *Physics Lett. A.* 342, 347-352.

[14] Pokutnyi, S.I., (2007). Exciton states in semiconductor quantum dots in the framework of the modified effective mass method. *Semiconductors.* 41, 1323-1331.

[15] Pokutnyi, S.I., (2010). Exciton states in semiconductor quantum dots. *Semiconductors.* 44, 488-493.

[16] Pokutnyi, S.I., (2012). Exciton states in semiconductor nanosystems. *Semiconductors.* 46, 174-184.

[17] Soloviev, V., Eeichofer, A., (2001). Approximation of effective mass in nanosystems. *Physica Status Solidi B*. 224, 285-291.

[18] Yeh, C., Zhang, S., Zunger, A., (2004). The effective mass method in nanosystems. *Physical Review B*. 62, 14408-14416.

[19] Bondar, N., Brodyn, M., (2010). Spectroscopy of semiconductor quantum dots. *Physics E*. 42, 1549-1555.

[20] Pokutnyi, S.I., (2013). Binding energy of the exciton of a spatially separated electron and hole in quasi-zero-dimensional semiconductor nanosystems. *Technical Physics Letters.* 39, 233-235.

[21] Pokutnyi, S.I., (2013). On an exciton with a spatially separated electron and hole in quasi-zero-dimensional semiconductor nanosystems. *Semiconductors.* 47, 791 -798.

[22] Pokutnyi, S.I., (2014). Theory of excitons formed from spatially separated electrons and holes in quasi-zero-dimensional semiconductor nanosystems. *SOP Transactions Theoretical Physics.* 1, 24 -35.

[23] Pokutnyi, S.I., (2013). Biexcitons formed from spatially separated electrons and holes in quasi-zero-dimensional semiconductor nanosystems. *Semiconductors.* 47, 1626-1635.

[24] Pokutnyi, S.I., (2014). Quasi-zero-dimensional nanostructures: Excitonic quasimolecules. *J. Appl. Chem*. 2, 1- 4.

[25] Efremov, N.A., Pokutny, S.I., (1985). Macroscopic local charge states in ultradispersion media. *Sov. Phys. Solid. State*. 27, 27- 35.

[26] Efremov, N.A., Pokutny, S.I., (1990). Energy spectrum of exciton in spherical particle. *Sov. Phys. Solid. State.* 32, 955- 964.

[27] Pokutnyi, S.I., (1992). Size quantization of electron-hole pair in semiconductor quantum dots. *Physics Lett. A.* 168, 433-438.

[28] Pokutnyi, S.I., (2011). Theory of exciton states in semiconductor nanosystems. *Physics Express*. 1, 158-164.

[29] Pokutnyi, S.I., Gorbyk, P.P., (2013). Superatoms in quasi-zero-dimensional nanostructures (review). *Progr. Phys. Metal*. 14, 144 - 168.

[30] Pokutnyi, S.I., Gorbyk, P.P., (2013). Superatoms in quasi-zero-dimensional nanosystems. *J. Appl. Chem*. 1, 44 - 47.

[31] Pokutnyi, S.I., (2012). Exciton states in quasi-zero-dimensional semiconductor nanosystems: Theory. *Phys. Express*. 2, 20 - 26.

[32] Pokutnyi, S.I., (2013). Exciton states in quasi-zero-dimensional nanostructures. *J. Appl. Chem*. 1, 5 - 18.

[33] Lozovik, Y., Nishanov, V., (1976). Exciton Wannier-Mott near the interface. *Physics Solid State*. 18, 1905-1911.

[34] Keldysh, L., (1979). The interaction of the electrons in a thin films. *Journal Experimental Theoretical Physics Letters*. 29, 621-624.

[35] Frish, S.E., (1963). Optical spectra of atoms. Nauka, Moscow [in Russian].